CrystEngComm

Accepted Manuscript

ROYAL SOCIETY OF CHEMISTRY

www.rsc.org/crystengcomm

12-Hydroxystearic Acid SAFiNs in Aliphatic Diols– A Molecular Oddity

Yaqi Lan[a] and Michael A. Rogers[b]

[a] Department of Food Science, Rutgers University, New Brunswick, NJ, 08901, USA.
[b] Department of Food Science, University of Guelph, Guelph, Ontario, Canada, N1G2W1

Abstract

12-Hydroxystearic acid (12-HSA), a structurally simple and cost-effective low molecular weight organogelator, has been studied extensively. It is established that the primary intermolecular interaction for self-assembly of 12-HSA molecular gels is hydrogen bonding and to a lesser extent van der Waals interactions. Due to the solvent-gelator interplay, it is expected that more polar solvents, especially hydrogen-bonding rich solvents are more likely to dissolve 12-HSA preventing gelation or crystallization. Surprisingly, it is found that 12-HSA is able to gelate a series of diols, but not their mono functional alcohols. A potential gelation mechanism is proposed that the diol co-crystallizes between 12-HSA molecules promoting 1-dimensional growth. The gelation behavior, fiber morphology, thermal properties as well as viscolastic properties of the resultant gels are drastically affected by the structure of diol solvents. Solvents shorter in chain length, with –OH groups at each terminal end, tend to form fibrous aggregates with higher gelation capacity, higher melting points and mechanically are stronger. Both increasing the diol chain length and the position of the hydroxyl groups from the primary positions lead to reduced gelation ability. The resultant gels comprised of highly branched, 'spherulitic-like' crystals are mechanically weaker with lower melting point.

Introduction

There is a growing body of literature being compiled on molecular gels in recent years due to fundamental insights garnered into 1-dimensional (1D) self-assembly processes.[1, 2] Despite being mostly liquid, molecular gels exhibit viscoelastic 'solid-like' properties with potential applications ranging from serving as structuring agents for cosmetics[3] and controlled drug release,[4-6] to structuring edible oils.[7, 8] The gels are based on a 3-dimensional (3D) network of randomly entangled or highly branched fibrous and/or platelet-like structures, resulting from the spontaneous self-assembly of individual low molecular mass organic gelators (LMOGs). Non-covalent interactions leading to the conversion of 0-dimensional (0D) objects to 1D and eventually 3D aggregates within molecular gels include hydrogen bonding[9-11], π-π stacking, and van der Waals interactions.[12] The gelation process is meticulous; governed by an intricate balance of forces of divergent origins, including interactions that assist dissolution of the gelator molecules and the intermolecular forces, which promote epitaxial growth into 1D elongated aggregates.[13-15] In another words, gelation relies on a balance between solvent-gelator and gelator-gelator interactions.[16-22] Optimal gelation is typically achieved when the solvent-gelator interaction is limited and the self assembled fibrillar networks (SAFiNs) are comprised of thin entangled fibers. [23]

12-Hydroxystearic acid (12-HSA) has been widely studied,[17, 19, 20, 24-33] due to its inexpensive cost, simple structure and superior gelation capacity. 12-HSA stabilizes its aggregates via London dispersion force and H-bonding interactions. In optically pure R- or L-12-HSA, the hydroxyl groups at the chiral center of 12-HSA are linked via unidirectional hydrogen bonds resulting in helical aggregates.[34] Early work indicated that SAFiN formation of 12-HSA

results from the dimerization of carboxylic acid head group and formation of hydrogen bonding array between the secondary hydroxyl groups.[32, 35, 36]

The solvent-gelator interplay influences the gelation behavior of 12-HSA. When solvent-gelator interactions increase and compete with gelator-gelator interactions, the probability of forming thicker fibers increases.[20, 23, 37] Further increasing the solvent-gelator interactions result in solubilization of gelator. It has been reported that the gelation of 12-HSA is closely related to hydrogen bonding Hansen solubility parameter (δ_h) of the solvent. In less polar solvents, where δ_h is lower than 4.7 MPa, clear gels formed, solutions remained in more polar solvents when δ_h is greater than 5.1 MPa, and opaque gels were obtained in between when $4.7 < \delta_h > 5.1$ MPa.[25] The nanostructure, microstructure and supramolecular structure of 12-HSA molecular gels are also influenced by solvent structure.[20] Alkanes and thiols produced transparent gels that are comprised of fibrillar aggregates of higher crystallinity; while nitriles, aldehydes, and ketones yield opaque gels with spherulitic supramolecular crystalline network.

Due to the nature of 12-HSA, presence of H-bonding rich solvents may lead to enhanced solvent-gelator interaction that restrict gelator-gelator interactions and disrupt the self-assembly of 12-HSA limiting organogel formation, i.e., monofunctional alcohols formed solutions with 12-HSA.[24, 25] Interestingly, it was found that a very polar solvent ethylene glycol (δ_h = 26 $Mpa^{0.5}$) formed gels rather than solutions when 12-HSA was added,[24] which might indicate a completely different gelation mechanism. It is likely that the solvent molecules are incorporated into SAFiN supramolecular structure and may serve as a 'bridge' between gelator molecules. In order to gain a better understanding of this interesting phenomenon, a series of short chain mono- and di-functional alcohols were examined to see how they influence the self-assembly behavior of 12-HSA as well as their micro and nanostructures.

Materials and Methods

Gelation test

12-HSA and 11 alcohols (Table 1) (Sigma-Aldrich, St. Louis, MO, USA) were used as received for the gelation test, with a minimum purity of 95%. 12-HSA was dispersed in each solvent at 0.1 wt%, 0.5 wt%, 1 wt%, 2 wt%, 3 wt%, 4 wt% and 5 wt%. Each sample was prepared in closed vials with Teflon liners (VWR, Allentown, PA, USA) and heated to 95 ^oC in water bath for 20 min, then cooled down and stored at 20 ^oC for 24 hrs. Inverted tube technique was utilized to determine the final material state.[38] The vial was inverted for 1 hr and if the material did not flow it was considered as a gel. The critical gelator concentration (CGC) was defined as the lowest gelator concentration tested that impeded flow for a specific solvent and 12-HSA combination.

Table 1: Gelation results for mono-ols and diols used as solvents and their corresponding δ_h. Gels are represented by their critical gelator concentration (CGC). S represents solution. P represents precipitate.

Solvent	Structure	δ_h ($Mpa^{0.5}$)	CGC (wt%)
1,2-Ethanediol	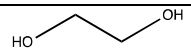	26	1
1-Propanol	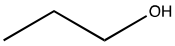	17.4	S
2-Propanol	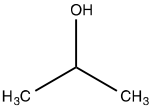	16.4	S
1,2-Propanediol	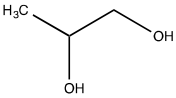	23.3	3
1,3-Propanediol	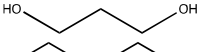	23.2	1
1-Butanol	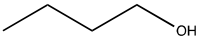	15.8	S
2-Butanol	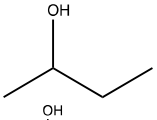	14.5	S
1,3-Butanediol	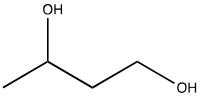	21.5	5
1,4-Butanediol	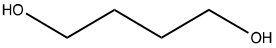	21.7	3
1-Pentanol	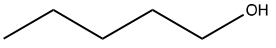	13.9	S
1,5-Pentanediol	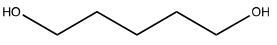		4

Polarized light microscopy
Polarized light micrographs were obtained using a imagining station (Linkham, Surrey, England) equipped with a Q imaging 2560×1920 pixel CCD camera (Micropublisher, Surrey, Canada) and a 10× Olympus lens (0.25 N.A.) (Olympus, Tokyo, Japan). Samples (3 wt%) were placed on a glass slide and immediately covered with a cover slip and imaged.

Rheological measurements
The rheological properties of all gels (concentration varied from the CGC to 5 wt%) were assessed using a Discovery H2 hybrid rheometer (TA Instruments, New Castle, DE) with an 8 mm stainless steel cross-hatched parallel plate geometry and a temperature-controlled stainless steel Peltier plate (New Castle, DE, USA). Samples were prepared in rheological molds that are made of Swagelok compression fittings (**Figure 1**) to prevent solvent evaporation at high temperatures. The samples obtained from the molds were 7 mm thick with a diameter of 12 mm. A frequency sweep was conducted from 0.1 to 50 Hz at constant strain of 1%, followed by an oscillatory stress sweep with a frequency of 1 Hz at 20 ^{o}C from 1 to 5000 Pa or until the gel yielded, triggering an over-speed error.

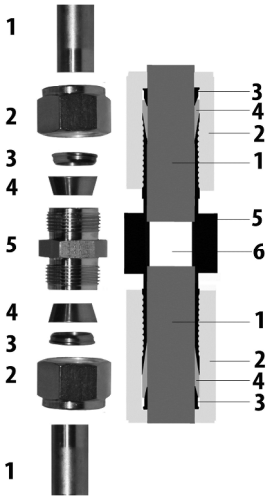

Figure 1: Rheological molds constructed from 2 Swagelok compression fittings: (1) stainless steel rod, (2) compression nut, (3) outer compression ring, (4) inner compression ring, (5) threaded fitting body, (6) 700 μm (length) x 1200 μm (diameter) gel chamber.

Differential scanning calorimetry (DSC)
A Q2000 differential scanning calorimeter (DSC) (TA instruments, New Castle, DE, USA) was utilized to measure the melting point and transition enthalpy. The DSC chamber was pre-cooled to 20 ^{o}C with a nitrogen flush (50 ml/min). 6 to 10 mg of gel samples (concentration varies from the CGC to 5 wt%) were sealed in hermetic aluminum DSC pans and heated to 95 ^{o}C at 5 ^{o}C/min, then held isothermally for 10 min, and then were cooled down to 20 ^{o}C at 5 ^{o}C/min. TA analysis software (TA Instruments, New Castle, DE, USA) was used to integrate the transition peaks to determine the onset melting temperature and melting enthalpy.

X-ray diffraction (XRD)
A Rigaku Multiflex Powder X-ray Diffractometer (Rigaku, Japan) with a ½^{o} divergence slit, ½^{o} scatter slit, and a 0.3 mm receiving slit, was set at 40 kV and 44 mA to determine the polymorphic form of the 12HSA networks. Scans were performed from 1 to 30 ^{o} at 0.2 ^{o}/min.

Results and discussions

All of the mono-functional alcohol solvents (1-propanol, 2-propanol, 1-butanol, 2-butanol and 1-pentanol) formed solutions upon cooling (**Table 1**). This observation agrees with previous studies, indicating that 12-HSA is unable to form molecular gels in solvents with δ_h higher than 6.5 MPa$^{0.5}$.[25] The inability to form SAFiNs is due to the strong hydrogen bonding interaction between solvent and gelator molecules that compete with inter-gelator H-bonding (**Figure 2**)[20] and disrupts SAFiN formation of 12-HSA.

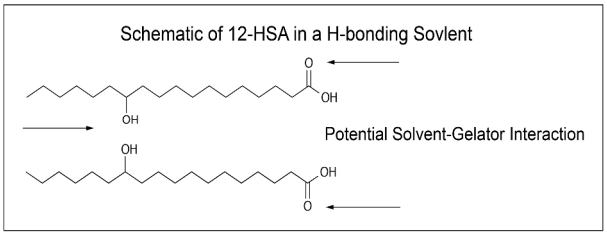

Figure 2: Schematic representation of 12-HSA in a H-bonding solvent.

However, recently it was found that diols, used as the solvent, formed gels with varying CGC. The CGCs are relatively high compared to 12-HSA in other less polar solvents where the CGC are usually near 1%. None of the alcohols tested form a gel using 12-HSA under 1wt%. Diols with shorter aliphatic chains and with primary hydroxyl groups at each end tend to have lower CGC compared to diols with a primary and secondary alcohol, which indicates greater gelling ability. Changing the hydroxyl position and increasing the aliphatic chain length of solvents reduced the gelation capacity of 12-HSA.

Early work using 12-HSA showed that SAFiN formation results from the dimerization of the carboxylic acid head group and formation of hydrogen bonding array between the secondary hydroxyl groups promoting the 1D epitaxial growth.[32, 35, 36] With the presence of a hydroxyl-rich solvent, it is inevitable that solvent molecules form H-bonds with 12-HSA restricting 1D growth (**Figure 2**) resulting in solvation. A speculated explanation for the gelation of diols is that solvent molecules are inserted between hydrogen bonding arrays of two gelator molecules and serves as a 'bridge', allowing the 1D epitaxial growth to still progress. As solvent molecules are able to form H-bonding with both the primary carboxylic acid head group as well as the secondary hydroxyl group, the dimerization of 12-HSA is restricted resulting in reduced gelation capacity, which may cause higher CGCs compared to other solvents. In order to foster a better understanding of the potential gelation mechanism, micro and nanostructures as well as the viscoelastic properties and state transition behavior of the resultant gels are characterized.

All the gels formed are visually opaque. The transparency of molecular gels has been correlated to the morphology of aggregates formed, the number of junction zones as well as the number and the cross-sectional thickness of the crystalline aggregates within the self-assembled network.[39, 40] The larger the constitute of a SAFiN network, the more opaque the gel appears. Polarized light microscopy (**Figure 3**) was utilized to examine the morphology of the

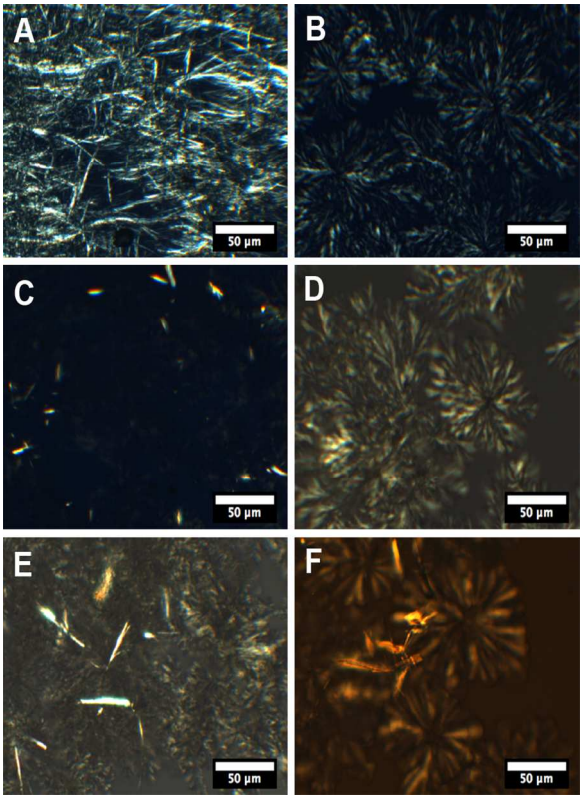

Figure 3: Polarized light micrographs of 3 wt% 12-HSA in 1,2-ethanediol (A), 1,2-propanediol (B), 1,3-propanediol (C), 1,3-butanediol (D), 1,4-butanediol (E) and 1,5-pentanediol (F). The scale bar is 50 µm.

crystalline aggregates of the supramolecular network within gels. The shape of the aggregates for 1,2-ethanediol, 1,3-propanediol and 1,4-butanediol are drastically different than in 1,2-propanediol, 1,3-butanediol and 1,5-pentanediol. 1,2-ethanediol, 1,3-propanediol and 1,4-butanediol tend to form fibrous aggregates that are less branched. These three solvents share a molecular similarity in that each are symmetric with two hydroxyl groups attached at the ends of the aliphatic chain. These solvents allow for the formation of aggregates with higher aspect ratios and are more effective at entrapping liquid, corresponding to lower CGC (**Table 1**). With an increase in chain length, the fibers formed become thicker and shorter with reduced gelling capability. The morphology of gels from 1,2-propanediol, 1,3-butanediol and 1,5-pentanediol (**Figure 3**) indicates the presence of fewer nuclei and fibers grow in a radial fashion with a higher branching rate resulting in a 'spherulitic-like'

appearance and the polymorphic crystalline structure of the neighboring 12HSA domains interpenetrate or could may adapt a molecular tilt to immobilize solvent. The morphology of this type of self-assembled network is less effective resulting in higher CGCs (**Table 1**). It is not surprising that when the solvent is being incorporated as 'bridging' molecule between gelator molecules, both the increase in chain length and sub-optimal configuration result in 12-HSA not effectively dimerizing via their carboxyl groups before being incorporated into the crystal lattice. As a result, crystal imperfections are enhanced, impeding 1D epitaxial crystal growth and the frequency of fiber tip branching.

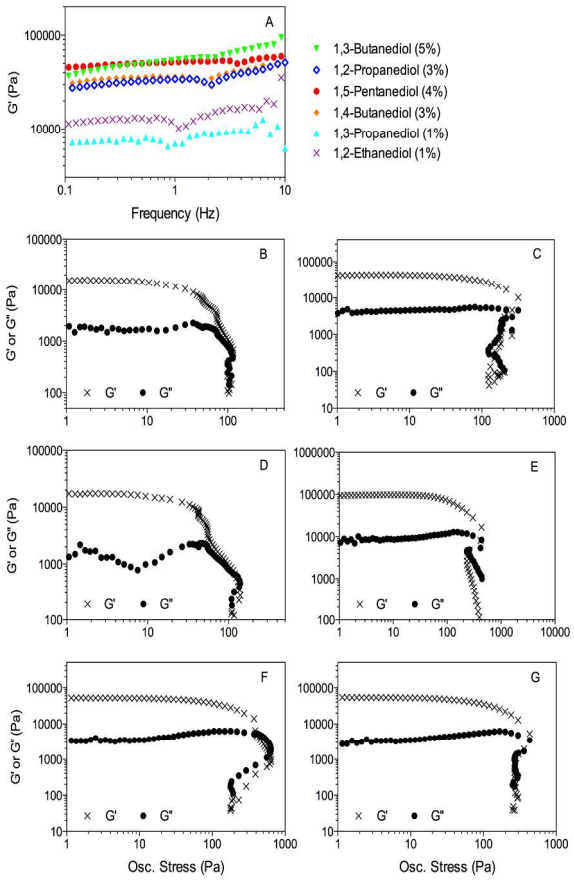

Figure 4: Frequency sweep of 12-HSA molecular gels in various alcohol solvents at their CGC (A), and the corresponding oscillatory stress sweep at each CGC for 1,2-ethanediol (B), 1,2-propanediol (C), 1,3-propanediol (D), 1,3-butanediol (E) 1,4-butanediol (F) and 1,5-pentanediol.

The viscoelastic properties of the organogels were characterized using small deformation oscillatory rheology. Rheological measurements confirmed the gel formation at the CGC for each alcohol solvent, where storage modulus (G′) is greater than the loss modulus (G″) over a broad range of frequencies (**Figure 4A**). Further, G′ is higher G″ within linear viscoelastic region (LVR) for the solvents tested at CGC (**Figure 4B**), indicating a 'solid-like' behavior. The morphology of the SAFiN network determines the rheological properties of the gel. Usually, the elastic properties are dependent on the amount of solids, the spatial distribution of mass and the nature of crystal-crystal interactions.[41] The gel strength, characterized by G′, increases with an increase in concentration for both 1,2-ethanediol and 1,3-propanediol (**Figure 5**).

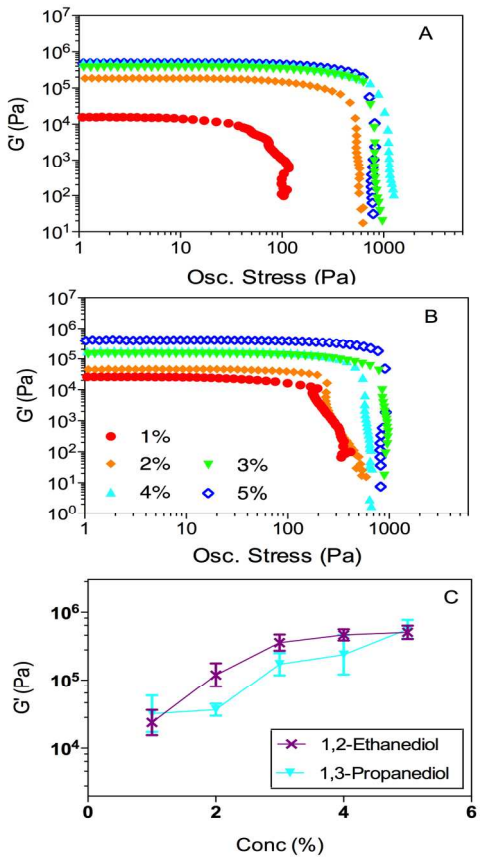

Figure 5: Influence of concentration on storage modulus (G′) of 12-HSA molecular gels in 1,2-ethanediol (A) and 1,3-propanediol (B). Plot C shows mean with error of G′ as a function of 12-HSA concentrations for solvents as labeled.

Overall, 1,2-ethanediol exhibits a slightly higher gel strength than 1,3-propanediol, due to the shorter aliphatic chain length. To examine the influence of chain length and position of –OH group, rheological experiments for all the solvents at a fixed gelator concentration (5%) were conducted (**Figure 6**). The corresponding G′, G″ and yield stress illustrate drastically different physical properties of the gels (**Table 2**). As the oscillatory stress increases, the gel yields and G′ becomes lower than G″, i.e., exhibits "liquid-like" behavior, which is characterized by yield stress of a gel. Albeit the effect of chain length is not linear on the viscoelastic properties, the diols with shorter aliphatic chains and with –OH groups attached on end position (1,2-ethanediol and 1,3-propanediol) tend to generate mechanically stronger gels with higher G′ and higher yield stress (**Table 2**). This trend in rheological properties can be explained by their SAFiN morphologies (**Figure 3**). The stronger networks are attributed to the formation of longer and thinner fibers with larger aspect ratios that are more effective at entrapping solvent via surface tension and capillary forces.[42, 43] Increases in chain length and sub-optimal configuration of –OH groups trigger the crystal formation in a sub-optimal fashion and results in shorter, thicker fibers or highly branched "spherulitic-like" crystals that are less effective at immobilizing solvent leading to weaker gels.

The profile of the state transition was determined using DSC. 1,2-propanediol, 1,3-butanediol, 1-4-butanediol and 1,5-pentanediol did not show crystallization peaks. Only melting thermograms was presented after 24 hrs of storage at 20 °C (**Figure 7**). The lack of crystallization peak is due to the slow crystallization process of 12-HSA in these solvents. This is consistent with the proposed gelation mechanism when solvent molecule is incorporated into SAFiN structure. When the aliphatic chain length increases and hydroxyl groups are not located on the end positions, it is more difficult for solvent molecules to orient linking two 12-HSA molecules.

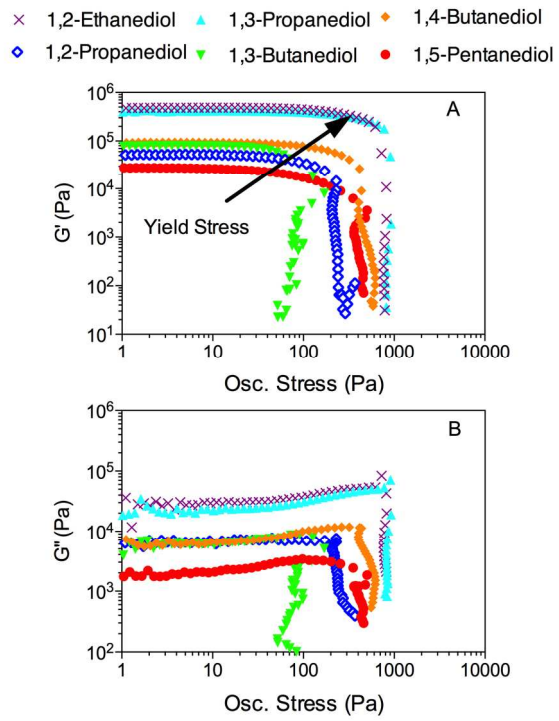

Figure 6: Influence of solvent structure on storage modulus (G′), loss modulus (G″) and yield stress for 5 wt% 12-HSA molecular gels. The yield stresses were determined when *G′* decreased to < 90% of the average value determined from the linear viscoelastic region of the gels.

Table 2: Storage modulus (G′), loss modulus (G″) and yield stress of 5 wt% 12-HSA molecular gels in various diols.

	G′ (Pa)	G″ (Pa)	Yield stress (Pa)
1,2-Ethanediol	$5.1\times10^{5} \pm 1.2\times10^{5}$	$3.8\times10^{5} \pm 1.3\times10^{5}$	209 ± 44
1,2-Propanediol	$5.0\times10^{4} \pm 1.9\times10^{3}$	$5.8\times10^{3} \pm 7.3\times10^{2}$	74 ± 2
1,3-Propanediol	$5.6\times10^{5} \pm 2.0\times10^{5}$	$3.0\times10^{4} \pm 7.8\times10^{3}$	265 ± 10
1,3-Butanediol	$8.6\times10^{4} \pm 9.6\times10^{3}$	$8.3\times10^{3} \pm 2.0\times10^{3}$	53 ± 9
1,4-Butanediol	$9.6\times10^{4} \pm 7.4\times10^{3}$	$6.3\times10^{3} \pm 2.2\times10^{2}$	126 ± 11
1,5-Pentanediol	$2.5\times10^{4} \pm 5.9\times10^{3}$	$1.7\times10^{3} \pm 2.4\times10^{2}$	40 ± 4

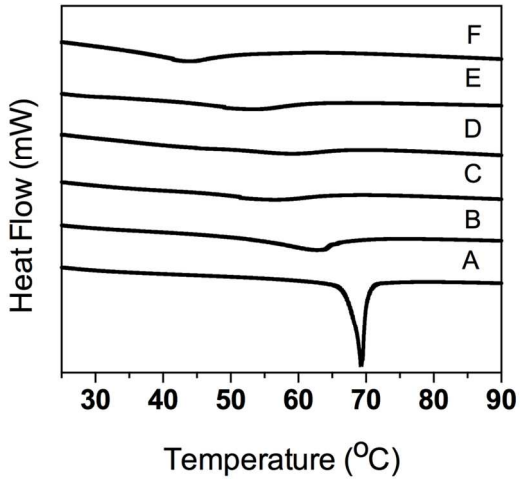

Figure 7: Thermograms for the melting transition of 12-HSA molecular gels in 1,2-ethanediol (A), 1,3-propanediol (B), 1,4-butanediol (C), 1,5-pentanediol (D), 1,2-propanediol (E) and 1,3-butanediol (F).

The melting profile for 12-HSA molecular gels in various di-functional alcohols shows that only 1,2-ethanediol exhibits a sharp melting peak. The broad peaks from other diols indicate greater number of crystal imperfections. The "degree of crystallinity" is also reflected in the melting temperature, which is typically influenced by crystallographic mismatches, solvent inclusion and degree of annealing (i.e., less crystalline imperfections). The melting temperature is affected by the gelator concentration (**Figure 8A**), while melting enthalpy is proportional to the amount of gelator added within the system (**Figure 8B**). The length of diol and the position of hydroxyl groups on diols affect the onset temperature and melting enthalpy (**Figure 9**). When examining the correlation between chain length and T_m for 1,2-ethanediol, 1,3-propanediol, 1,4-butanediol and 1,5-pentanediol, a significant decrease in T_m is observed, indicating that the crystal imperfection is enhanced with increasing chain length. A decrease is also observed in melting enthalpy, but less significant. Due to the broadness of melting peaks, it is difficult to obtain an accurate measure of the area under curve, representing the enthalpy of melting, which may contribute to the poor correlation with H_m. By studying the melting properties of 1,2-propanediol and 1,3-propanediol or 1,3-butanediol and 1,4-butanediol molecular gels, the influence of the hydroxyl position can be assessed. The crystallinity of the SAFiN was greater when the two hydroxyl groups are located on the ends of the aliphatic chain. This coincides with the proposed gelation mechanism that when the solvent molecule are incorporated between 12-HSA molecules. When solvent has a longer aliphatic chain, there is more flexibility in the orientation of linker diol molecule resulting in higher probability of forming imperfect crystals. The entropy change ($\Delta S=\Delta H/T$) during gel-sol transition can be calculated from the melting enthalpy (ΔH_m) and melting temperature (T_m). The trend observed is similar to that of enthalpy change (**Figure 9C**). The entropy change for 1,2-ethanediol during sol-gel transition is significantly higher than that for the other diol solvents. It is not surprising as 1,2-ethanediol has the shortest chain length so the orientation of 1,2-ethanediol between gelator molecules is relatively fixed with little flexibility, resulting in a larger increase in the entropy during gel-sol transition.

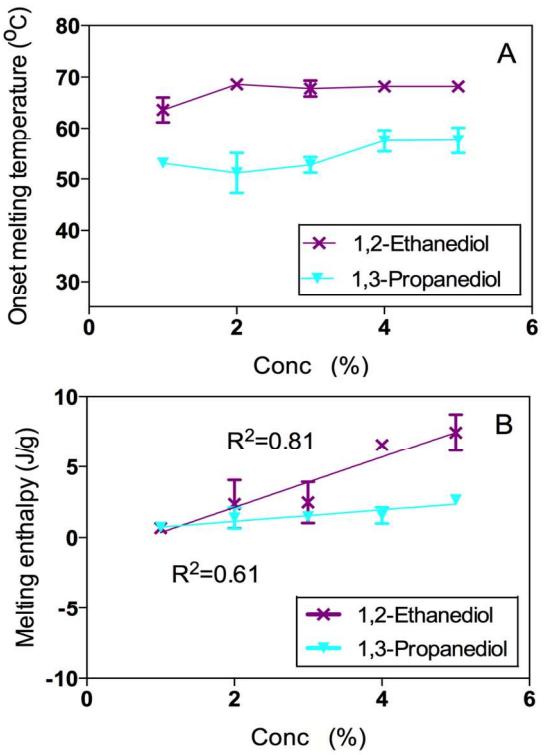

Figure 8: Onset melting temperature (T_m) and melting enthalpy (H_m) as a function of gelator concentration (%) for 1,2-ethanediol and 1,3-propanediol.

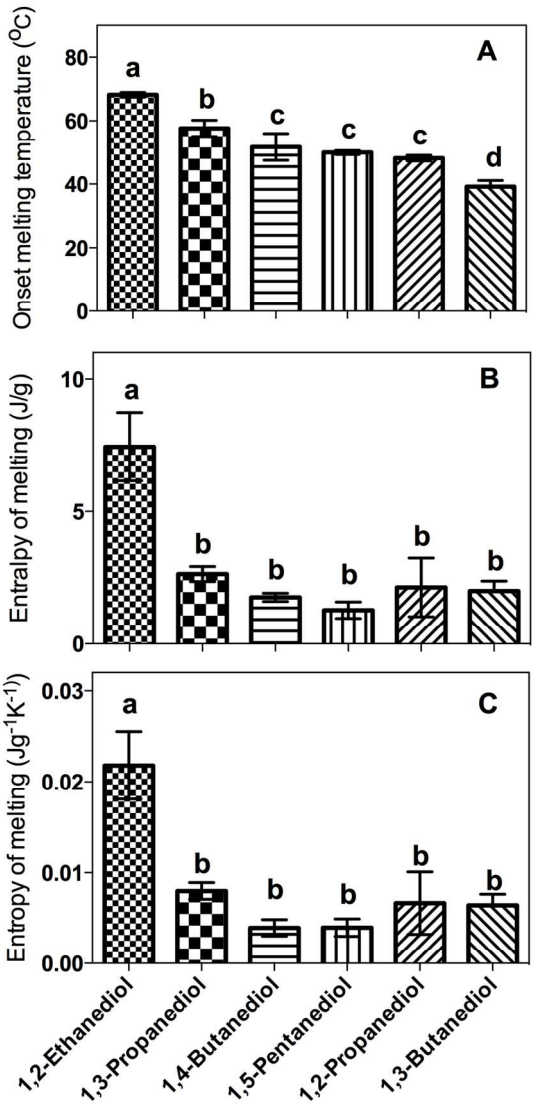

Figure 9: Melting onset temperature (A), melting enthalpy (B) and melting entropy (C) of 5 wt%12-HSA in various solvents. Statistical analysis was performed using one-way ANOVA ($p < 0.05$) and the labels a, b, c and d indicate statistical differences between the gels in various diols.

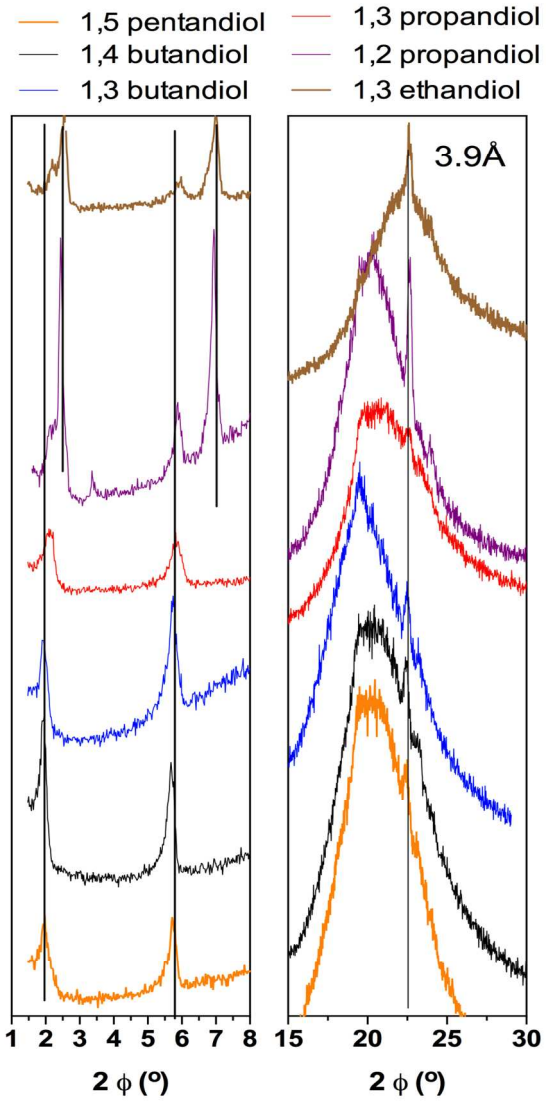

Figure 10: Vertically offset wide-angle (left) and small-angle (right) diffractograms for 5 wt% of 12-HSA in diols.

The change in macroscopic properties originates from either the micro and/or the nano structure of the SAFiNs. By correlating the result from polarized light microscopy (**Figure 3**), it was found that fibrous, less branched crystals have a higher melting points. Highly branched 'spherulitic-like' crystals tend to have lower melting point. The trend in melting temperature can be explained by crystallographic mismatch theory.[10, 44, 45] Crystallographic mismatches occur when gelator molecules are incorporated in a sub-optimal configuration onto the crystal lattice resulting in branch points. Shorter diols with hydroxyl groups at the ends are more effective at linking two 12-HSA molecules, leading to more crystalline fibrillar aggregates with higher melting points. As the diols becomes less effective as acting as a 'bridge' molecule due to increase aliphatic chain or/and sub-optimal configuration of –OH groups, mismatches occur resulting in decreased fiber

length and enhanced branching, thus, lower melting point.

With drastic difference in microstructures, rheological properties and melting profiles, the nanostructure of gels were probed by measuring the wide-angle and small-angle spacing of 12-HSA gels in various diols. The X-ray diffractograms (**Figure 10**) for 1,2-ethanediol and 1,2-propanediol exhibit similar diffraction patterns with a wide-angle spacing of 44.8 Å and 38.3 Å and *hlk* higher order reflections at 15.1 Å and 12.8 Å suggesting two distinct "polymorphic" morphologies. The peaks for 1,3-propanediol, 1,3-butanediol, 1,4-butanediol and 1,5-pentanediol are only at 44.8 Å and a *hlk* higher order reflection at 15.1 Å. The wide-angle spacing varies between 38.2 to 44.8 Å, which is slightly shorter than the bimolecular length of extended 12-HSA molecules (46 Å), indicating an interdigitated packing of gelator molecules.[32] The single d-spacing (3.9 Å) from small-angle scattering (**Figure 10**) for all the gels approximately corresponds to the hexagonal packing of fatty acid chains within a layer (~4.1 Å).[41] The broad peak between 15 ° and 25 ° is the amorphous scatter of the solvent. According to the results discussed above, a possible gelation mechanism includes a solvent molecule potentially being inserted between the secondary hydroxyl groups of 12-HSA, serving as a "bridge" that is still capable of promoting 1D fiber growth. If the diol is incorporated between the carboxylic acid head groups the wide-angle spacing would likely be greater than the bimolecular length of 12-HSA (46 Å), which is not the case as discussed.

Conclusions

It has been reported that 12-HSA is able to gel ethylene glycol (1,2-ethanediol),[24] however up until now no study has been done to examine the gelation mechanism behind it and if gel properties are influenced by the aliphatic chain length and/or the configuration of the hydroxyl groups. In this study, the gelation behavior, fiber morphology, thermal properties and viscolastic properties of the resultant gels were assessed, and a potential gelation mechanism proposed. This study demonstrates that the molecular packing in aggregates of structurally simple molecules, such as 12-HSA, from the nano to micro to macro levels, are drastically influenced by the nature of the diol solvents used in this study, which do not follow the same rules outlined by general solubility parameters.

---

* Corresponding author:
Email: mroger09@uoguelph.ca
Tel: + 519-824-4120 ext 54327

Reference

1. P. Terech and R. G. Weiss, *Chem. Rev.*, 1997, 97, 3133-3159.
2. N. M. Sangeetha and U. Maitra, *Chemical Society Reviews*, 2005, 34, 821-836.
3. J. A. Morales-Rueda, E. Dibildox-Alvarado, M. A. Charó-Alonso, R. G. Weiss and J. F. Toro-Vazquez, *European Journal of Lipid Science and Technology*, 2009, 111, 207–215.
4. A. Friggeri, B. L. Feringa and J. van Esch, *Journal of Controlled Release*, 2004, 97, 241-248.
5. R. Kumar and O. P. Katare, *AAPS PharmSciTech*, 2005, 6, E298–E310.
6. T. Pénzesa, G. Blazsób, Z. Aignera, G. Falkayb and I. Erősa, *International journal of pharmaceutics*, 2005, 298, 47-54.
7. M. Pernetti, K. F. van Malssen, E. Floter and A. Bot, *Current Opinion in Colloid & Interface Science*, 2007, 12, 221-231.
8. F. AlHassawi and M. A. Rogers, *Journal of the American Oil Chemists Society*, 2013, 90, 1533-1540.
9. N. Yan, Z. Xu, K. K. Diehn, S. R. Raghavan, Y. Fang and R. G. Weiss, *Journal of the American Chemical Society*, 2013, 135, 8989-8999.
10. X. Y. Liu and P. D. Sawant, *Adv. Mater.*, 2002, 14, 421-426.
11. R.-Y. Wang, P. Wang, J.-L. Li, B. Yuan, Y. Liu, L. Li and X.-Y. Liu, *Physical Chemistry Chemical Physics*, 2013, 15, 3313-3319.
12. D. Farbi, J. Guan and A. Cesaro, *Thermochim. Acta*, 1998, 321, 3-16.
13. L. A. Estroff and A. D. Hamilton, *Chemical Reviews*, 2004, 104, 1202-1217.
14. R. G. Weiss and P. Terech, *Molecular Gels. Materials with Self-Assembled Fibrillar Networks*, Springer, Dordrecht The Netherlands, 2006.
15. M. Suzuki, Y. Nakajima, M. Yumoto, M. Kimura, H. Shirai and K. Hanabusa, *Langmuir : the ACS journal of surfaces and colloids*, 2003, 19, 8622-8624.

16. Y. Wu, S. Wu, G. Zou and Q. Zhang, *Soft Matter*, 2011, 7, 9177-9183.
17. M. A. Rogers and A. G. Marangoni, *Langmuir : the ACS journal of surfaces and colloids*, 2009, 25, 8556-8566.
18. A. R. Hirst, I. A. Coates, T. R. Boucheteau, J. F. Miravet, B. Escuder, V. Castelletto, I. W. Hamley and D. K. Smith, *Journal of the American Chemical Society*, 2008, 130, 9113-9121.
19. J. Gao, S. Wu, T. J. Emge and M. A. Rogers, *CrystEngComm*, 2013, 15, 4507.
20. S. Wu, J. Gao, T. J. Emge and M. A. Rogers, *Soft Matter*, 2013, 9, 5942.
21. Y. Lan, M. G. Corradini, X. Liu, T. E. May, F. Borondics, R. G. Weiss and M. A. Rogers, *Langmuir : the ACS journal of surfaces and colloids*, 2014, 30, 14128-14142.
22. Y. Lan, M. G. Corradini and M. A. Rogers, *Crystal Growth & Design*, 2014, 14, 4811-4818.
23. G. Zhu and J. S. Dordick, *Chemistry of Materials*, 2006, 18, 5988-5995.
24. M. Burkhardt, S. Kinzel and M. Gradzielski, *Journal of Colloid & Interface Science*, 2009, 331, 514–521.
25. J. Gao, S. Wu and M. A. Rogers, *Journal of Materials Chemistry*, 2012, 22, 12651.
26. M. A. Rogers and A. G. Marangoni, *Crystal Growth & Design*, 2008, 18, 4596-4601.
27. M. A. Rogers, A. K. Smith, A. J. Wright and A. G. Marangoni, *Journal of the American Oil Chemists Society*, 2007, 84, 899-906.
28. M. A. Rogers and R. G. Weiss, *New Journal of Chemistry*, 2015, 39, 785-799.
29. M. A. Rogers, A. J. Wright and A. G. Marangoni, *Food Research International*, 2008, 41, 1026-1034.
30. M. A. Rogers, A. J. Wright and A. G. Marangoni, *Current Opinion in Colloid & Interface Science*, 2009, 14, 33-42.
31. T. Sakurai, Y. Masuda, H. Sato, A. Yamagishi, H. Kawaji, T. Atake and K. Hori, *Bulletin of the Chemical Society of Japan*, 2010, 83, 145-149.
32. S. Wu, J. Gao, Emge. T. and M. A. Rogers, *Crystal Growth & Design*, 2013, 13, 1360-1366.
33. J. F. Toro-Vazquez, J. Morales-Rueda, A. Torres-Martínez, M. A. Charo-Alonso, V. A. Mallia and R. Weiss, G., *Langmuir : the ACS journal of surfaces and colloids*, 2013, 29, 7642-7654.
34. V. A. Mallia and R. G. Weiss, *Journal of Physical Organic Chemistry*, 2014, 27, 310-315.
35. V. A. Mallia, M. George, D. L. Blair and R. G. Weiss, *Langmuir : the ACS journal of surfaces and colloids*, 2009, 25, 8615-8625.
36. S. Abraham, Y. Lan, R. S. H. Lam, D. A. S. Grahame, J. J. H. Kim, R. G. Weiss and M. A. Rogers, *Langmuir : the ACS journal of surfaces and colloids*, 2012, 28, 4955-4964.
37. T. Pinault, B. Isare and L. Bouteiller, *CHEMPHYSCHEM*, 2006, 7, 816-819.
38. S. R. Raghavan and B. H. Cipriano, *Gel Formation: Phase Diagrams Using Tabletop Rheology and Calorimetry*, Springer, Netherlands, 2006.
39. P. Terech, D. Pasquier, V. Bordas and C. Rossat, *Langmuir : the ACS journal of surfaces and colloids*, 2000, 16, 4485-4494.
40. T. Tamura and M. Ichikawa, *Journal of the American Oil Chemists Society*, 1997, 74, 491-495.
41. T. S. Awad, M. A. Rogers and A. G. Marangoni, in *Fat Crystal Networks*, ed. A. G. Marangoni, Marcel Dekker, New York, 2005, pp. 1-20.
42. W. Edwards, C. A. Lagadec and D. K. Smith, *Soft Matter*, 2011, 7, 110-117.
43. J. G. Hardy, A. R. Hirst and D. K. Smith, *Soft Matter*, 2012, 8, 3399-3406.
44. R. Wang, X. Liu, J. Xiong and J. Li, *Journal of Physical Chemistry B*, 2006, 110, 7275-7280.
45. X.-L. Liu and P. D. Sawant, *CHEMPHYSCHEM*, 2002, 3, 374-377.